01 May 1999

Effects of Resonant Tunneling in Electromagnetic Wave Propagation through a Polariton Gap

Lev I. Deych

Alexey Yamilov
Missouri University of Science and Technology, yamilov@mst.edu

Alexander A. Lisyansky

Recommended Citation

L. I. Deych et al., "Effects of Resonant Tunneling in Electromagnetic Wave Propagation through a Polariton Gap," *Physical Review B (Condensed Matter)*, vol. 59, no. 17, pp. 11339-11348, American Physical Society (APS), May 1999.
The definitive version is available at https://doi.org/10.1103/PhysRevB.59.11339

Effects of resonant tunneling in electromagnetic wave propagation through a polariton gap

Lev I. Deych
Department of Physics, Seton Hall University, South Orange, New Jersey 07079

A. Yamilov and A. A. Lisyansky
Department of Physics, Queens College of City University of New York, Flushing, New York 11367

(Received 6 July 1998; revised manuscript received 9 November 1998)

We consider tunneling of electromagnetic waves through a polariton band gap of a one-dimensional chain of atoms. We analytically show that a defect embedded in the structure gives rise to the resonance transmission at the frequency of a local polariton state associated with the defect. Numerical Monte Carlo simulations are used to examine properties of the electromagnetic band arising inside the polariton gap due to finite concentration of defects. [S0163-1829(99)03418-9]

I. INTRODUCTION

The resonant tunneling of electromagnetic waves through different types of optical barriers is a fast developing area of optical physics. This effect was considered for photonic crystals,[1,2] where forbidden band gaps in the electromagnetic spectrum form optical barriers. Macroscopic defects embedded in the photonic crystal give rise to local photon modes,[3–7] which induce the resonant transmission of electromagnetic waves through the band gaps.

A different type of photonic band gaps arises in polar dielectrics, where a strong resonance interaction between the electromagnetic field and dipole active internal excitations of a dielectric brings about a gap between different branches of polaritons. Recently it was suggested that regular microscopic impurities embedded in such a dielectric give rise to local polariton states,[8–10] where a photon is coupled to an intrinsic excitation of a crystal, and both these components are localized in the vicinity of the defect.[11] The main peculiarity of the local polaritons is that their electromagnetic component is bound by a *microscopic* defect whose size is many order of magnitude smaller then the wavelengths of respective photons. Another important property of these states is the absence of a threshold for their appearance even in three-dimensional (3D) isotropic systems, while for all other known local states the ''strength'' of a defect must exceed a certain critical value before the state would split off a continous spectrum. The reason for this peculiar behavior is a strong van Hove singularity in the polariton density of states in the long-wave region, caused by a negative effective mass of the polariton-forming excitations of a crystal.

The feasibility of resonant electromagnetic tunneling induced by local polaritons, however, is not self-evident. The idea of a microscopic defect affecting propagation of waves with macroscopic wavelength seems to be in contradiction with common wisdom. Besides, it was found that the energy of the electromagnetic component of local polaritons is very small compared to the energy of its crystal counterpart. The existence of the tunneling effect was first numerically demonstrated in Ref. 9, where a 1D chain of dipoles interacting with a scalar field imitating transverse electromagnetic waves was considered. It was found that a single defect embedded in such a chain results in near 100% transmission at the frequency of local polaritons through a relatively short chain (50 atoms). The frequency profile of the transmission was found to be strongly assymetric, in contrast to the case of electron tunneling.[16]

In most cases (at least for a small concentration of the transmitting centers) one-dimensional models give a reliable description of tunneling processes, because by virtue of tunneling, a wave propagates along a chain of resonance centers, for which a 1D topology has the highest probability of occurrence.[17] In our situation, it is also important that the local polariton states (transmitting centers) occur without a threshold in 3D systems as well as in 1D systems. This ensures that the transmission resonances found in Ref. 9 are not artifacts of the one-dimensional nature of the model, and justifies a further development of the model. In the present paper we pursue this development in two interconnected directions. First, we present an exact analytical solution of the transmission problem through the chain with a single defect. This solution explains the unusual asymmetric shape of the transmission profile found in numerical calculations[9] and provides insight into the phenomenon under consideration. Second, we carry out numerical Monte Carlo simulation of the electromagnetic transmission through a macroscopically long chain with a finite concentration of defects, and study the development of a defect-induced electromagnetic pass band within the polariton band gap. The analytical solution of a single-defect model allows us to suggest a physical interpretation for some of the peculiarities of the transmission found in numerical simulations. As a by product of our numerical results we present an algorithm used for the computation of the transmission. This algorithm is based upon a blend of the transfer-matrix approach with ideas of the invariant-embedding method,[18] and proves to be extremely stable even deep inside the band gap, where traditional methods would not work.

Though we consider the one-dimensional model, the results obtained are suggestive for experimental observation of the predicted effects. Actually the damping of the electromagnetic waves is more experimentally restrictive than the topology of the system. We, however, discuss the effects due to damping and come to the conclusion that the effects under

discussion can be observed in regular ionic crystals in the region of their phonon-polariton band gaps.

The paper is organized as follows. The Introduction is followed by an analytical solution of the transmission problem in a single-impurity situation. The next section presents results of Monte Carlo computer simulations. The algorithm used in numerical calculations is derived and discussed in the Appendix. The paper concludes with a discussion of the results.

II. DESCRIPTION OF THE MODEL AND ANALYTICAL SOLUTION OF A SINGLE-DEFECT PROBLEM

A. The model

Our system consists of a chain of atoms interacting with each other and with a scalar ''electromagnetic'' field. Atoms are represented by their dipole moments P_n, where the index n represents the position of an atom in the chain. Dynamics of the atoms is described within the tight-binding approximation with an interaction between nearest neighbors only,

$$(\Omega_n^2-\omega^2)P_n+\Phi(P_{n+1}+P_{n-1})=\alpha E(x_n), \tag{1}$$

where Φ is a parameter of the interaction, and Ω_n^2 represents the site energy. Impurities in the model differ from host atoms in this parameter only, so

$$\Omega_n^2=\Omega_0^2 c_n+\Omega_1^2(1-c_n), \tag{2}$$

where Ω_0^2 is the site energy of a host atom, Ω_1^2 describes an impurity, c_n is a random variable taking values 1 and 0 with probabilities $1-p$ and p, respectively. Parameter p, therefore, sets the concentration of the impurities in our system. This choice of the dynamical equation corresponds to excitonlike polarization waves. Phononlike waves can be presented in a form that is similar to Eq. (1) with $\Omega_n^2=\Omega_0^2+(1-c_n)(1-M_{\rm def}/M_{\rm host})\omega^2$, where $M_{\rm def}$ and $M_{\rm host}$ are masses of defects and host atoms, respectively.

Polaritons in the system arise as collective excitations of dipoles (polarization waves) coupled to the electromagnetic wave $E(x_n)$, by means of a coupling parameter α. The electromagnetic subsystem is described by the following equation of motion:

$$\frac{\omega^2}{c^2}E(x)+\frac{d^2E}{dx^2}=-4\pi\frac{\omega^2}{c^2}\sum_n P_n\delta(na-x), \tag{3}$$

where the right-hand side is the polarization density caused by atomic dipole moments, and c is the speed of light in vacuum. The coordinate x in Eq. (3) is along the chain with an interatomic distance a. Equations (1) and (3) present a *microscopic* description of the transverse electromagnetic waves propagating along the chain in the sense that it does not make use of the concept of the dielectric permeability, and takes into account all modes of the field including those with wave numbers outside of the first Brillouin band.

This approach enables us to address several general questions. A local state is usually composed of states with all possible values of wave number k. States with large k cannot be considered within a macroscopic dielectric function theory, and attempts to do so lead to divergent integrals that need to be renormalized.[15] In our approach, all expressions are well defined, so we can check whether a contribution from large k is important, and if the long-wave approximation gives reliable results. Calculation of the integrals appearing in the 3D theory requires detailed knowledge of the spectrum of excitations of a crystal throughout the entire Brillouin band. This makes analytical consideration practically unfeasible. In our 1D model, we can carry out the calculations analytically (in a single-impurity case) and examine the influence of different factors (and approximations) upon the frequency of a local state and the transmission coefficient. Using caution, the results obtained can be used to assess approximations in 3D cases.

B. A single impurity problem

The equation for the frequency of the local polariton state in the 1D chain has a form similar to that derived in Ref. 8

$$1=\Delta\Omega^2 G(0), \tag{4}$$

where, however, the expression for the polariton Green's function $G(n-n_0)$ responsible for the mechanical excitation of the system can be obtained in the explicit form

$$G(n-n_0)=\sum_k \frac{\cos(ak)-\cos(a\omega/c)}{[\omega^2-\Omega_0^2-2\Phi\cos(ka)][\cos(ak)-\cos(a\omega/c)]-\dfrac{2\pi\alpha\omega}{c}\sin(a\omega/c)}\exp[ik(n-n_0)a]. \tag{5}$$

If one neglects the term responsible for the coupling to the electromagnetic field, the Green's function $G(n-n_0)$ is reduced to that of the pure atomic system. This fact reflects the nature of the defect in our model: it only disturbs the mechanical (not related to the interaction with the field) properties of the system. A solution of Eq. (4) can be real valued only if it falls into the gap between the upper and lower polariton branches. This gap exists if the parameter Φ in the dispersion equation of the polariton wave is positive, and the effective mass of the excitations in the long-wave limit is, therefore, negative.

The diagonal element $G(0)$ of Green's function (5) can be calculated exactly. The dispersion equation (4) then takes the following form:

$$1=\Delta\Omega^2\frac{1}{2\Phi D(\omega)}\left[\frac{\cos(a\omega/c)-Q_2(\omega)}{\sqrt{Q_2^2(\omega)-1}}-\frac{\cos(a\omega/c)-Q_1(\omega)}{\sqrt{Q_1^2(\omega)-1}}\right], \tag{6}$$

where $Q_{1,2}(\omega)$,

$$Q_{1,2}(\omega)=\frac{1}{2}\left[\cos\left(\frac{a\omega}{c}\right)+\frac{\omega^2-\Omega_0^2}{2\Phi}\right]\pm\frac{1}{2}D(\omega), \tag{7}$$

$$D(\omega)=\sqrt{\left[\cos\left(\frac{a\omega}{c}\right)-\frac{\omega^2-\Omega_0^2}{2\Phi}\right]^2-\frac{4\pi\alpha\omega}{\Phi c}\sin\left(\frac{a\omega}{c}\right)} \tag{8}$$

give the poles of the integrand in Eq. (5). The bottom of the polariton gap is determined by the condition $D(\omega)=0$, yielding in the long-wave limit, $a\omega/c\ll 1$, for the corresponding frequency ω_l,

$$\omega_l^2\simeq\tilde{\Omega}_0^2-2\tilde{\Omega}_0^2 d\frac{\sqrt{\Phi}a}{c}, \tag{9}$$

where we introduce parameters $d^2=4\pi\alpha/a$, $\tilde{\Omega}_0^2=\Omega_0^2+2\Phi$, and take into account that the bandwidth of the polarization waves Φ obeys the inequality $\sqrt{\Phi}a/c\ll 1$. The last term in this expression is the correction to the bottom of the polariton gap due to the interaction with the transverse electromagnetic field. Usually this correction is small, but it has an important theoretical, and, in the case of strong enough spatial dispersion and oscillator strength, practical significance.[8] Because of this correction the polariton gap starts at a frequency, when the determinant $D(\omega)$ becomes imaginary, but functions $Q_{1,2}(\omega)$ are still less than 1. This leads to the divergence of the right-hand side of Eq. (6) as ω approaches ω_l, and, hence, to the absence of a threshold for the solution of this equation. This divergence is not a 1D effect since the same behavior is also found in 3D isotropic model.[8,10] An asymptotic form for Eq. (6) when $\omega\to\omega_l$ in the 1D case reads

$$\sqrt{\omega^2-\omega_l^2}\sim\frac{\Delta\Omega^2}{\sqrt{\Phi}}, \tag{10}$$

and differs from the 3D case by the factor of $(d\omega_l a)/(c\sqrt{\Phi})$. The upper boundary of the gap $\omega_{\rm up}$ is determined by the condition $Q_1(\omega)=0$, leading to

$$\omega_{\rm up}^2=\tilde{\Omega}_0^2+d^2, \tag{11}$$

Eq. (6) also has a singularity as $\omega\to\omega_{\rm up}$, but this singularity is exclusively caused by the 1D nature of the system. We will discuss local states that are not too close to the upper boundary in order to avoid manifestations of purely 1D effects.

For frequencies deeper inside the gap, Eq. (4) can be simplified in the approximation of small spatial dispersion, $\sqrt{\Phi}a/c\ll 1$, to yield

$$\omega^2=\tilde{\Omega}_1^2-\Delta\Omega^2\left[1-\sqrt{\frac{\omega^2-\tilde{\Omega}_0^2}{\omega^2-\tilde{\Omega}_0^2+4\Phi}}\right]-d^2\frac{\omega a}{2c}\frac{\Delta\Omega^2}{\sqrt{(\omega^2-\tilde{\Omega}_0^2)(\tilde{\Omega}_0^2+d^2-\omega^2)}}, \tag{12}$$

where $\tilde{\Omega}_1^2=\Omega_1^2+2\Phi$ is a fundamental ($k=0$) frequency of a chain composed of impurity atoms only. Two other terms in Eq. (12) present corrections to this frequency due to the spatial dispersion and the interaction with the electromagnetic field, respectively. One can see that both corrections have the same sign and shift the local frequency into the region between $\tilde{\Omega}_0^2$ and $\tilde{\Omega}_1^2$. As we see below, this fact is significant for the transport properties of the chain.

Transmission through the system can be considered in the framework of the transfer matrix approach. This method was adapted for the particular case of the system under consideration in Ref. 9. The state of the system is described by the vector v_n, with components P_n, P_{n+1}, E_n, E_n'/k_ω, which obeys the following difference equation:

$$v_{n+1}=T_n v_n. \tag{13}$$

The transfer matrix T_n describes the propagation of the vector between adjacent sites:

$$T_n=\begin{pmatrix} 0 & 1 & 0 & 0\\ -1 & -\dfrac{\Omega_n^2-\omega^2}{\Phi} & \dfrac{\alpha}{\Phi}\cos ka & \dfrac{\alpha}{\Phi}\sin ka\\ 0 & 0 & \cos ka & \sin ka\\ 0 & -4\pi k & -\sin ka & \cos ka \end{pmatrix}. \tag{14}$$

Analytical calculation of the transmission coefficient in the situation considered is not feasible even in the case of a single impurity because the algebra is too cumbersome. The problem, however, can be simplified considerably if one neglects the spatial dispersion of the polarization waves. In this case the T matrix can be reduced to a 2×2 matrix of the following form:

$$\tau_n=\begin{pmatrix} \cos ka & \sin ka\\ -\sin ka+\beta_n\cos ka & \cos ka+\beta_n\sin ka \end{pmatrix}, \tag{15}$$

where the parameter β_n

$$\beta_n=\frac{4\pi\alpha\omega}{c(\omega^2-\Omega_n^2)}, \tag{16}$$

represents the polarizability of the nth atom due to its vibrational motion. In this case the complex transmission coefficient t can be easily expressed in terms of the elements of the resulting transfer matrix, $T^{(N)}=\Pi_1^N\tau_n$,

$$t=\frac{2}{(T_{11}^{(N)}+T_{22}^{(N)})-i(T_{12}^{(N)}-T_{21}^{(N)})}e^{-ikL}. \tag{17}$$

The problem is, therefore, reduced to the calculation of $T^{(N)}$. In the case of a single impurity, the product of the transfer

matrices, τ, can be presented in the following form:

$$T^{(N)} = \tau^{N-n_0} \times \tau_{\mathrm{def}} \times \tau^{n_0-1}, \tag{18}$$

where the matrix τ_{def} describes the impurity atom with $\Omega_n = \Omega_1$. The matrix product in Eq. (18) is conveniently calculated in the basis, where the matrix τ is diagonal. After some cumbersome algebra, one obtains for the complex transmission coefficient:

$$t = \frac{2e^{ikL}\exp(-\kappa L)}{[1 - i/\sqrt{R}(2-\beta\cot ka)][(1+\varepsilon)] + 2i\exp(-\kappa L)\Gamma\cosh[\kappa a(N-2n_0+1)]}, \tag{19}$$

where $R = \beta^2 + 4\beta\cot(ak) - 4$, $\Gamma = \varepsilon\beta/[\sin(ka)\sqrt{R}]$, κ is the imaginary wave number of the evanescent electromagnetic excitations, which determines the inverse localization length of the local state, and $\varepsilon = (\beta_{\mathrm{def}} - \beta)/2\sqrt{R}$. The last parameter describes the difference between host atoms and the impurity, and is equal to

$$\varepsilon = \frac{2\pi\alpha}{c\sqrt{R}}\omega\frac{(\Omega_1^2 - \Omega_0^2)}{(\omega^2 - \Omega_0^2)(\omega^2 - \Omega_1^2)}. \tag{20}$$

We have also neglected here a contribution from the second eigenvalue of the transfer matrix, which is proportional to $\exp(-2\kappa L)$, and is exponentially small for sufficiently long chains. For $\varepsilon = 0$, Eq. (19) gives the transmission coefficient, t_0, of the pure system,

$$t_0 = \frac{2e^{ikL}\exp(-\kappa L)}{1 - i/\sqrt{R}(2-\beta\cot ka)}, \tag{21}$$

exhibiting a regular exponential decay. At the lower boundary of the polariton gap Ω_0, parameters β and κ diverge, leading to vanishing transmission at the gap edge regardless the length of the chain. It is instructive to rewrite Eq. (19) in terms of t_0:

$$t = \frac{t_0}{(1+\varepsilon) + i\exp(-ikL)\Gamma t_0\cosh[\kappa a(N-2n_0+1)]}. \tag{22}$$

This expression describes the resonance tunneling of the electromagnetic waves through the chain with the defect. The resonance occurs when

$$1 + \varepsilon = 0, \tag{23}$$

the transmission in this case becomes independent of the system size. Substituting the definition of the parameter ε given by Eq. (20) into Eq. (23), one arrives at an equation identical to Eq. (12) for the frequency of the local polariton state with the parameter of the spatial dispersion Φ being set to zero. The transmission takes a maximum value when the defect is placed in the middle of the chain, $N - 2n_0 + 1 = 0$, and in this case

$$|t_{\max}|^2 = \frac{1}{\Gamma^2} \leqslant 1. \tag{24}$$

The width of the resonance is proportional to Γt_0 and decreases exponentially with an increase of the system's size. In the long-wave limit, $ak \ll 1$, Eq. (24) can be rewritten in the following form:

$$|t_{\max}|^2 = 1 - \left(1 - 2\frac{\omega_r^2 - \Omega_0^2}{d^2}\right), \tag{25}$$

where ω_r is the resonance frequency satisfying Eq. (23). It is interesting to note that the transmission coefficient becomes exactly equal to one if the resonance frequency happens to occur exactly in the center of the polariton gap. This fact has a simple physical meaning. For $\omega_r^2 = \Omega_0^2 + d^2/2$ the inverse localization length κ becomes equal to the wave number ω_r/c of the incoming radiation. Owing to this fact, the field and its derivative inside the chain exactly match the field and the derivative of the incoming field as though the optical properties of the chain are identical to those in vacuum. Consequently, the field propagates through the chain without reflection.

Having solved the transmission problem we can find the magnitude of the field inside the chain in terms of the incident amplitude E_{in} at the resonance frequency. Spatial distribution of the field in the local polariton state can be found to have the form $E = E_d\exp(-|n - n_0|\kappa a)$. Matching this expression with the outcoming field equal to $E_{\mathrm{in}}t\exp(ikL)$ one has for the field amplitude at the defect atom, E_d,

$$E_d = E_{\mathrm{in}}t\exp(-ikL)\exp[(N - n_0)\kappa a]. \tag{26}$$

For $|t|$ being of the order of one in the resonance this expression describes the drastic exponential enhancement of the incident amplitude at the defect side due to the effect of the resonance tunneling.

Equations (22) and (24) demonstrate that the resonance tunneling via local polariton states is remarkably different from other types of resonance tunneling phenomena, such as electron tunneling via an impurity state,[16] or through a double barrier. The most important fact is that the frequency profile of the resonance does not have the typical symmetric Lorentzian shape. At $\omega = \Omega_1$ the parameter ε diverges causing the transmission to vanish. At the same time the resonance frequency ω_r is very close to Ω_1 as it follows from Eq. (12). This results in strongly asymmetric frequency dependence of the transmission, which is skewed toward lower frequencies.

The transmission vanishes precisely at two frequencies: at the low-frequency band edge Ω_0 and at the frequency Ω_1 associated with the vibrational motion of the defect atom. At the same time, the behavior of the transmission coefficient in the vicinities of these two frequencies is essentially different: at the band edge it is $(\omega^2-\Omega_0^2)^2\exp(-1/\sqrt{\omega^2-\Omega_0^2})$, while at the defect frequency the transmission goes to zero as $(\omega^2-\Omega_1^2)^2$. These facts can be used to predict several effects that would occur with the increase of the concentration of the defects. First, one can note that with the increase of concentration of the impurities frequency Ω_1 becomes eventually the boundary of the new polariton gap when all the original host atoms will be replaced by the defects atoms. One can conclude then that the zero of the transmission at Ω_1 instead of being washed out by the disorder, would actually become more singular. More exactly one should expect that the frequency dependence of the transmission in the vicinity of Ω_1 will exhibit a crossover from the simple power decrease to the behavior with exponential singularity associated with the band edge. Second, if one takes into account such factors as spatial dispersion or damping, which prevent transmission from exact vanishing, one should expect that the above-mentioned crossover to the more singular behavior would manifest itself in the form of substantial decrease of the transmission in the vicinity of Ω_1 with an increase of the concentration. Numerical calculations discussed in the next section of the paper show that this effect does take place even at rather small concentration of the defects.

Resonance tunneling is very sensitive to the presence of relaxation, which phenomenologically can be accounted for by adding $2i\gamma\omega$ to the denominator of the polarizability β, where γ is an effective relaxation parameter. This will make the parameter ϵ complex valued, leading to two important consequences. First, the resonance condition becomes $\mathrm{Re}(\varepsilon)=-1$, and it can be fulfilled only if the relaxation is small enough. Second, the imaginary part of ε will prevent the exponential factor t_0 in Eq. (22) from canceling out at the resonance. This restricts the length of the system in which the resonance can occur and limit the enhancement of the field at the defect. These restrictions though are not specific for the system under consideration and affect experimental manifestation of any type of resonant tunneling phenomenon.

Since we are only concerned with a frequency region in the vicinity of Ω_1, real ε_1 and imaginary ε_2 parts of ε can be approximately found as

$$\varepsilon_1 \simeq d^2\frac{\Omega_1 a}{2c}\sqrt{\frac{\Delta\Omega^2}{d^2-\Delta\Omega^2}}\frac{\omega^2-\Omega_1^2}{(\omega^2-\Omega_1^2)^2+4\gamma^2\omega^2}, \quad (27)$$

$$\varepsilon_2 \simeq \frac{2\gamma\omega}{\omega^2-\Omega_1^2}\varepsilon_1. \quad (28)$$

It follows from Eq. (27) that the resonance occurs only if $(4\gamma c)/(ad^2)<1$. This inequality has a simple physical meaning: it ensures that the distance between the resonance frequency ω_r and Ω_1, where the transmission goes to zero, is greater than the relaxation parameter, γ. This is a rather strict condition that can only be satisfied for high-frequency oscillations with large oscillator strength in crystals with large interatomic spacing a. The spatial dispersion, however, makes conditions for the resonant tunneling much less restrictive. In order to estimate the effect of the dissipation in the presence of the spatial dispersion one can rely upon Eq. (22) assuming that the dispersion only modifies the parameter ε, but does not effect the general expression for the transmission. This assumption is justified by the numerical results of Ref. 9 and the present paper, which show that the transmission properties in the presence of the spatial dispersion do not differ significantly from the analytical calculations performed for the chain of noninteracting dipoles. According to Eq. (12), the interatomic interaction moves the resonance frequency further away from Ω_1 undermining the influence of the damping and leading to a weaker inequality: $(\gamma\Omega_1)/\Phi<1$. This condition can be easily fulfilled, even for phonons with a relatively small negative spatial dispersion. For the imaginary part ε_2 at the resonance one can obtain from Eq. (28) the following estimate:

$$\varepsilon_2 \sim \min[(4\gamma c)/(ad^2),(\gamma\Omega_1)/\Phi]. \quad (29)$$

The requirement that ε_2 be much smaller than t_0 leads to the following restriction for the length of the system $L \ll (1/\kappa)|\ln[\varepsilon_2]|$, with ε_2 given above. The maximum value of the field at the defect site attainable for the defect located in the center of the chain is then found as $|E_d|\sim|E_{\mathrm{in}}||t|/\sqrt{\varepsilon_2}$.

III. ONE-DIMENSIONAL DIPOLE CHAIN WITH FINITE CONCENTRATION OF IMPURITIES

In this section we present results of numerical Monte Carlo simulations of the transport properties of the system under consideration in the case of randomly distributed identical defects. If spatial dispersion is taken into account the regular Maxwell boundary conditions must be complemented by additional boundary conditions regulating the behavior of polarization P at the ends of the chain. In our previous paper[9] we calculated the transmission for two types of boundary conditions: $P_0=P_N=0$, which corresponds to the fixed ends of the chain, and $P_0=P_1$, $P_{N-1}=P_N$, which corresponds to the relaxed ends. We reported in Ref. 9 that the transmission is very sensitive to the boundary conditions with fixed ends being much more favorable for the resonance. Our present numerical results obtained with an improved numerical procedure and the analytical calculations do not confirm this dependence of the resonant tunneling upon the boundary conditions. In the case of a single impurity we find that for both types of the boundary conditions the transmission demonstrates sharp resonance similar to that found in Ref. 9 for fixed ends. Similarly, for a finite concentration of impurities we did not find any considerable differences in the transmission for both types of boundary conditions. We conclude that the actual form of the boundary conditions is not significant for the resonant tunneling.

The transfer matrix, Eq. (13), along with the definition of the transfer matrix, Eq. (14), and the boundary conditions chosen in the form of fixed terminal points, provides a basis for our computations. However, it turns out that straightforward use of Eq. (13) in the gap region is not possible because of underflow errors arising when one pair of eigenvalues of the transfer matrix becomes exponentially greater than the second one. In order to overcome this problem we develop a

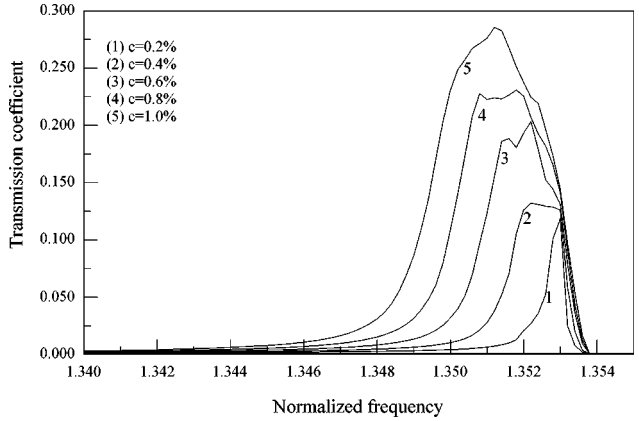

FIG. 1. Frequency dependence of the averaged transmission coefficient for small concentrations of the defects. The frequency is normalized by the fundamental ($k=0$) frequency of the pure chain, Ω_0. The low-frequency boundary of the polariton gap is at $\omega \approx 1.3$ and is not shown here.

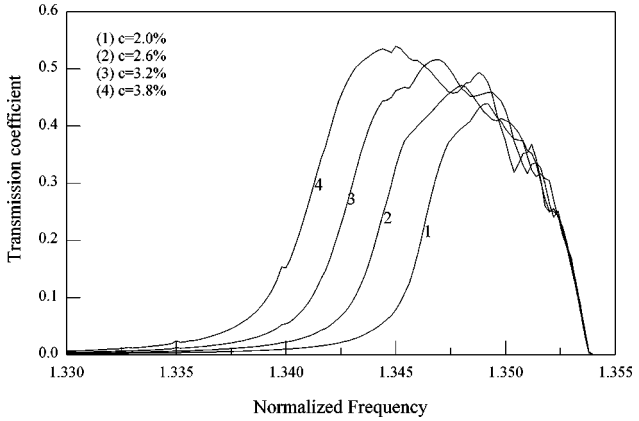

FIG. 2. The same as in Fig. 1 but for intermediate concentrations.

computational approach based upon the blend of the transfer-matrix method with the invariant embedding ideas. The central element of the method is a 4×4 matrix $S(N)$ that depends upon the system size N. The complex transmission coefficient t is expressed in terms of the elements of this matrix as

$$t=2\exp(-ikL)(S_{11}+S_{12}). \tag{30}$$

The matrix $S(N)$ is determined by the following nonlinear recursion:

$$S(N+1)=T_N\times\Xi(N)\times S(N), \tag{31}$$

where matrix $\Xi(N)$ is given by

$$\Xi(N)=\{I-S(N)\times H\times[I-T(N)]\}^{-1}. \tag{32}$$

The initial condition to Eq. (31) is given by

$$S(0)=(G+H)^{-1}, \tag{33}$$

where matrices G and H are specified by the boundary conditions. The derivation of Eqs. (30)–(33) and more detailed discussion of the method is given in the Appendix. The test of the algorithm based upon recursion formula (31) proves the method provides accurate results for transmission coefficients as small as 10^{-15}.

In our simulations we fix the concentration of the defects and randomly distribute them among the host atoms. The total number of atoms in the chain is also fixed; the results presented below are obtained for a chain consisting of 1000 atoms. For the chosen defect frequency, $\Omega_1\simeq1.354\Omega_0$, the localization length of the local polariton state l_{ind} is approximately equal to 150 interatomic distances. The transmission coefficient is found to be extremely sensitive to a particular arrangements of defects in a realization exhibiting strong fluctuations from one realization to another. Therefore, in order to reveal the general features of the transmission independent of particular positions of defects, we average the transmission over 1000 different realizations. We have also calculated the averaged Lyapunov exponent (the inverse localization length l_{chain} characterizing transport through the entire chain) to verify that the averaged transmission reveals a reliable information about the transport properties of the system.

The results of the computations are presented in the figures below. Figures 1 –3 show an evolution of the transmission with the increase of the concentration of the impurities. In Fig. 1 one can see the change of the transport properties at small concentrations up to 1%. The curve labeled (1) shows, basically, the single impurity behavior averaged over random positions of the defect. With an increase of the concentration there is a greater probability for two (or more) defects to form a cluster resulting in splitting a single resonance frequency in two or more frequencies. The double-peak structure of the curves (2) and (3) reflects these cluster effects. With the further increase of the concentration the clusters' sizes grow on average leading to multiple resonances with distances between adjacent resonance frequencies being too small to be distinguished. Curve (5) in Fig. 1 reflects this transformation, which marks a transition between individual tunneling resonances and the defect-induced band. The concentrations in this transition region is such that an average distance between the defects is equal to the localization length of the individual local states l_{ind}. The collective localization length at the frequency of the transmission peak $l_{\mathrm{chain}}^{\max}$ becomes equal to the length of the chain at approximately the same concentration that allows us to suggest a simple linear relationships between the two lengths. The nu-

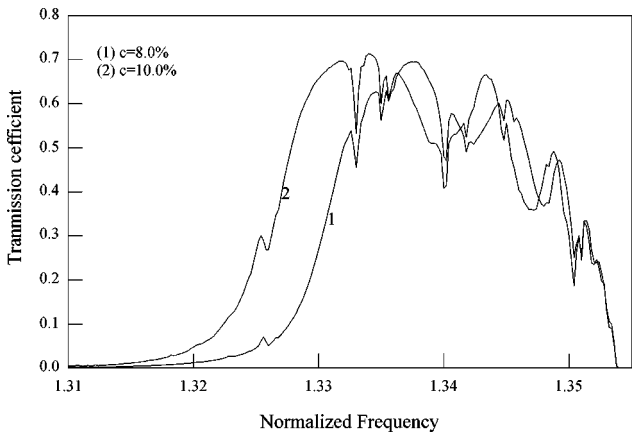

FIG. 3. The same as in Fig. 1 but for large concentrations.

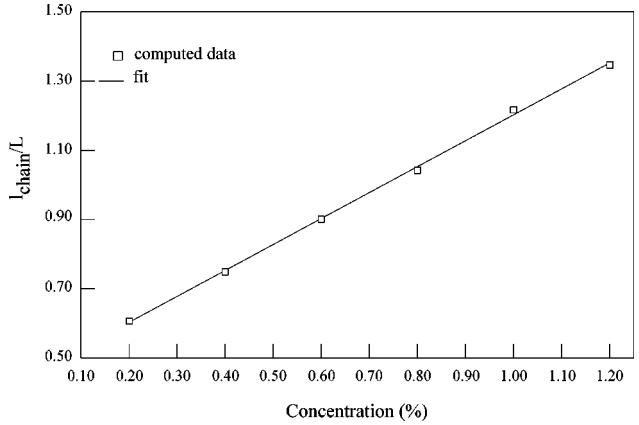

FIG. 4. Concentration dependence of the collective localization length l_{chain} normalized by the system's size L.

merical results presented in Fig. 4 clearly demonstrate this linear concentration dependence of $l_{\text{chain}}^{\max}$ at small concentrations. For larger concentrations one can see from Figs. 2 and 3 that the peak of the transmission coefficient develops into a broad structure. This marks further development of the defect pass band. Curves in Fig. 2 show the transmission coefficient at intermediate concentrations, where localization length l_{chain} is bigger than the length of the system only in a small frequency region around the maximum of the transmission, and Fig. 3 presents a well developed pass band with multipeak structure resulting from geometrical resonances at the boundaries of the system.

These figures reveal an important feature of the defect polariton band: its right edge does not move with increase of the concentration. The frequency of this boundary is exactly equal to the defect frequency Ω_1 (which is normalized by Ω_0 in the figures), and the entire band is developing to the left of Ω_1 in complete agreement with the arguments based upon an analytical solution of the single-impurity problem. Moreover, the magnitude of the transmission in the vicinity of Ω_1 decreases with an increase of the concentration also in agreement with our remarks at the end of the previous section. Figure 5 presents the inverse localization length l_{chain}, normalized by the length of the chain for three different concentrations. It can be seen that $l_{\text{chain}}^{-1}(\Omega_1)$ significantly grows

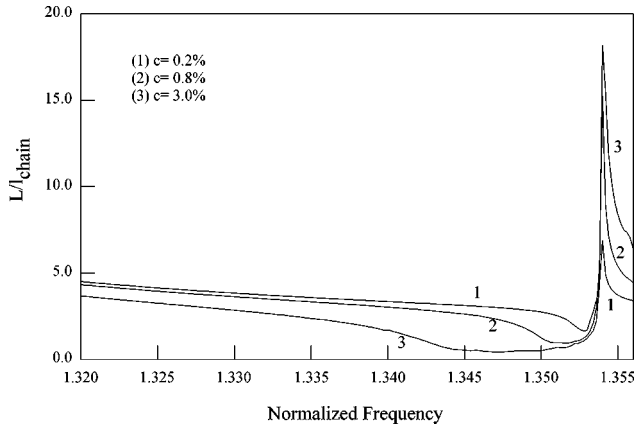

FIG. 5. Frequency dependence of the Lyapunov exponent of the entire chain for several concentrations in the frequency region of the defect band.

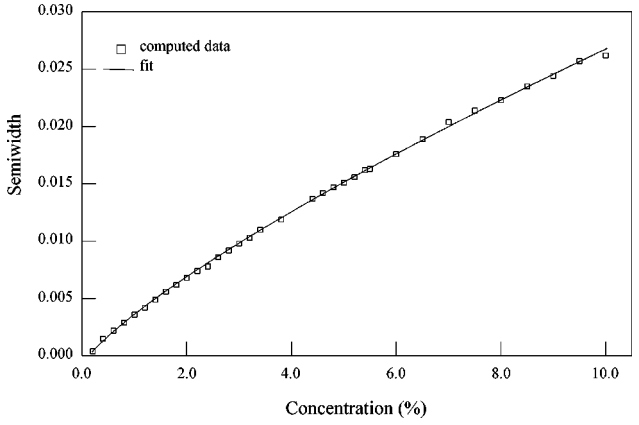

FIG. 6. Concentration dependence of the semiwidth of the defect band. The solid line represents fit with power function c^{ν}, where $\nu \approx 0.8$.

with an increase of the concentration, reaching the value of approximately $17/L$ at a concentration as small as 3%. Such a small localization length corresponds to the transmission of the order of magnitude of 10^{-17}, which is practically zero in our computation. Further increase of the concentration does not change the minimum localization length. These results present an interesting example of the defects building up a boundary of the forbidden gap.

This figure also shows the development of the pass band to the left of Ω_1 presented above in Figs. 1–3, but at a larger scale. We cannot distinguish here the details of the frequency dependence, but the transition from the single resonance behavior to the pass band, marked by the significant flattening of the curve, is clear.

Figure 6 presents the concentration dependence of the semiwidth δ_ω of the defect band. The semiwidth is defined as the difference between the frequency of the maximum transmission and the right edge of the band. One can see that all the points form a smooth line with no indication of a change of the dependence with the transition between different transport regimes. Attempts to fit this curve showed that it is excellently fitted by the power law $\delta_\omega \propto c^{\nu}$ with $\nu \simeq 0.8$ in all studied concentration range. The reason for this behavior and why it is insensitive to the change of the character of the transport requires further study.

IV. CONCLUSION

In this paper, we considered one-dimensional resonance tunneling of scalar ''electromagnetic waves'' through an optical barrier caused by a polariton gap. The tunneling is mediated by local polariton states arising due to defect atoms embedded in an otherwise ideal periodic chain. We also numerically studied how a defect-induced propagating band emerges from these resonances when the concentration of defects increases.

It is important to emphasize the difference between the situation considered in our paper and other types of tunneling phenomena discussed in the literature. The tunneling of electromagnetic waves through photonic crystals and electron tunneling, despite all the difference between these phenomena, share one common feature. In both cases, the resonance

occurs due to defects that have dimensions comparable with wavelengths of the respective excitations (electrons interact with atomic impurities, and long-wave electromagnetic waves interact with macroscopic distortions of the photonic crystals). In our case the wavelength of the propagating excitations is many orders of magnitude greater than dimensions of the atomic defects responsible for the resonance. The physical reason for such an unusual behavior lies in the nature of local polaritons. These states are formed owing to the presence of internal polariton-forming excitations. The spatial extent of these states is much larger than the geometrical dimensions of atomic defects and is comparable to the wavelength of the incident radiation.

We presented an exact analytical solution of the tunneling of electromagnetic waves through a chain of noninteracting atoms with a single defect. This solution provides insight into the nature of the phenomenon under consideration and allows one to obtain an explicit expression for the magnitude of the electromagnetic field at the defect site. The expression derived demonstrates that the field is strongly enhanced at the resonance with its magnitude growing exponentially with an increase of the length of the system. This effect is an electromagnetic analog of the charge accumulation in the case of electron tunneling, where it is known to cause interesting nonlinear phenomena.[19–23]

An analytical solution of the single-defect problem allowed us to make predictions regarding the transport properties of the system with multiple randomly located defects. The most interesting of these is that the dynamical frequency of the defects Ω_1, sets a high-frequency boundary for the defect-induced pass band, which does not move with increasing concentration of defects. Numerical Monte Carlo simulations confirmed this assumption and showed that the direct interaction between the atoms (spatial dispersion) does not affect resonance tunneling considerably, though it adds interesting features to it. One of them is the behavior of the transmission in the vicinity of Ω_1. In absence of the spatial dispersion, the transmission at this point is exactly equal to zero, and remains small when the interaction is taken into account. The interesting fact revealed by the numerical analysis is that the transmission at Ω_1 decreases with an increase in the concentration of the defects and nearly approaches zero at concentrations as small as 3%. This fact can be understood in light of the transfer-matrix approach: if the frequency Ω_1 corresponds to the eigenvalue of the defect's transfer matrix, which significantly differs from one, the transmission will diminish strongly each time the wave encounters a defect site, regardless the order in which the defects are located. Numerical results also demonstrated a transition between two transport regimes: one associated with resonance tunneling and the other occurring when the resonances spatially overlap and a pass band of extended states emerges. The transition occurs when the average distance between the defects becomes equal to the localization length of the single local state. At the same time the collective localization length at the peak transmission frequency, characterizing the transport properties of the entire chain, becomes equal to the total length of the system. This result assumes the linear dependence of this collective localization length upon concentration, which we directly confirm for small concentrations. Numerical results also showed that the width of the resonance, which develops into a pass band with an increase in concentration, does not manifest any transformation when the character of transport changes. The concentration dependence of the width was found to be extremely well described by a power law with an exponent approximately equal to 0.8. The nature of this behavior awaits an explanation.

APPENDIX: INVARIANT EMBEDDING ALGORITHM FOR THE TRANSFER-MATRIX EQUATION

In this appendix we develop an invariant embedding approach to transfer-matrix equations of a general form and deduce Eqs. (30)–(33) used for Monte Carlo calculations in our paper. We consider a typical difference equation of the transfer-matrix method,

$$u_{n+1}=T_n u_n, \tag{A1}$$

with boundary conditions of a general form:

$$Gu_0+Hu_N=v. \tag{A2}$$

Here u_n is a vector of an appropriate dimension that characterizes the state of the system at the nth site, T_n is a respective transfer matrix; G and H are matrices of the same dimension as the transfer matrix, together with the vector v they specify boundary conditions at the left and right boundaries of the system (cites 0 and N, respectively). The regular Maxwell boundary conditions and the fixed ends boundary condition for polarization can be presented in the form Eq. (A2) with the following matrices G,H, and vector v:

$$G=\begin{pmatrix} 1 & -i & 0 & 0 \\ 1 & -i & 0 & 0 \\ 0 & 0 & 1 & 0 \\ 0 & 0 & 1 & 0 \end{pmatrix}, \quad H=\begin{pmatrix} 1 & i & 0 & 0 \\ -1 & -i & 0 & 0 \\ 0 & 0 & 0 & 1 \\ 0 & 0 & 0 & -1 \end{pmatrix},$$

$$v=\begin{pmatrix} 2 \\ 2 \\ 0 \\ 0 \end{pmatrix}. \tag{A3}$$

These matrices are singular, but one should not worry about this, because we will only need to invert their sum, which has a nonzero determinant. In accordance with the ideas of the invariant embedding method[18] we consider the dynamic vector u_n as a function of the current site n, the length of the system N, and the boundary vector v:

$$u_n \equiv u(n,N,v) \equiv S(n,N)v. \tag{A4}$$

In the last equation we use the linear nature of Eq. (A1) in order to separate out the dependence upon the vector v. Substituting Eq. (A4) into Eqs. (A1) and (A2) we have the dynamical equation and boundary conditions for the matrix S:

$$S(n+1,N)=T_n \times S(n,N), \tag{A5}$$

$$G\times S(0,N)+H\times S(N,N)=I, \tag{A6}$$

where I is a unit matrix. The matrix $S(n,N+1)$, which describes the system with one additional scatterer, obviously satisfies the same equation (A5) as $S(n,N)$. Relying again upon the linearity of Eq. (A5) we conclude that $S(n,N)$ and $S(n,N+1)$ can only differ by a constant (independent of n) matrix factor $\Lambda(N)$:

$$S(n,N+1)=S(n,N)\times\Lambda(N). \tag{A7}$$

In order to find $\Lambda(N)$ we first substitute Eq. (A7) into boundary conditions Eq. (A6) which yield

$$\Lambda(N)=G\times S(0,N+1)+H\times S(N,N+1). \tag{A8}$$

Boundary conditions Eq. (A6) do not change if N is replaced by $N+1$, therefore we can write down that

$$G\times S(0,N+1)=I-H\times S(N+1,N+1). \tag{A9}$$

Substituting this expression into Eq. (A8) we have for the matrix $\Lambda(N)$:

$$\Lambda(N)=I+H\times[S(N,N+1)-S(N+1,N+1)]. \tag{A10}$$

The quantity $S(N+1,N+1)$ can be eliminated from this equation by means of Eq. (A1): $S(N+1,N+1)=T_N\ S(N,N+1)$, and we have for $\Lambda(N)$

$$\Lambda(N)=I+H\times[I-T(N)]\times S(N,N+1). \tag{A11}$$

Substituting this formula into Eq. (A7) we obtain the equation that governs the evolution of the matrix $S(n,N)$ with the change of the parameter N:

$$S(n,N+1)=S(n,N)+S(n,N)\times H\times[I-T(N)]\times S(N,N+1). \tag{A12}$$

This equation, however, is not closed because of an unknown matrix $S(N,N+1)$. This matrix can be found by setting $n=N$ in Eq. (A12):

$$S(N,N+1)=\{I-S(N,N)\times H\times[I-T(N)]\}^{-1}S(N,N). \tag{A13}$$

Introducing notation

$$\Xi(N)=\{I-S(N,N)\times H\times[I-T(N)]\}^{-1} \tag{A14}$$

the previous expression can be rewritten in the following compact form:

$$S(N,N+1)=\Xi(N)\times S(N,N). \tag{A15}$$

Inserting Eq. (A15) into Eq. (A12) we finally obtain

$$S(n,N+1)=S(n,N)+S(n,N)\times H\times[I-T(N)]\times\Xi(N)\times S(N,N). \tag{A16}$$

This equation still has an unknown quantity $S(N,N)$ which must be determined separately. We achieve this by combining the original transfer-matrix equation (A1) and Eq. (A15) to obtain the following:

$$S(N+1,N+1)=T_N\times\Xi(N)\times S(N,N). \tag{A17}$$

Equation (A17) is a nonlinear matrix equation with an initial condition given by

$$(G+H)\times S(0,0)=I. \tag{A18}$$

Equations (30)–(33) of the main body of the paper coincide with Eqs. (A16)–(A18) with simplifyed notation for the matrix S, where we dropped the second argument. They constitute the complete set of embedding equations for the transfer-matrix problem. In order to find the transmission coefficient one has to multiply the matrix $S(N,N)$ by the boundary vector v; the first component of the resulting vector is equal to $t\exp(ikL)$, where t is the complex transmission coefficient. If one is interested in the distribution of the state vector $u(n,N)$ throughout the entire system, one has to find $S(N,N)$ and then to solve Eq. (A16).

The presented algorithm was proved to be extremely stable, it produced reliable results for transmission as small as 10^{-17}. This stability is due to the operation of inversion involved in the calculations [see Eq. (A14)]. This operation prevents elements of the matrix S to grow uncontrollably in the course of the calculations.

[1] E. Yablonovitch, T. J. Gmitter, R. D. Meade, A. M. Rappe, K. D. Brommer, and J. D. Joannopoulos, Phys. Rev. Lett. **67**, 3380 (1991).

[2] J. D. Joannopoulos, R. D. Meade, and J. N. Winn, *Photonic Crystals: Molding the Flow of Light* (Princeton University Press, Princeton, NJ, 1995).

[3] E. Yablonovitch, Phys. Rev. Lett. **58**, 2059 (1987).

[4] R. D. Meade, K. D. Brommer, A. M. Rappe, and J. D. Joannopoulos, Phys. Rev. B **44**, 13 772 (1991).

[5] D. R. Smith, R. Dalichaouch, N. Kroll, S. Schultz, S. L. McCall, and P. M. Platzman, J. Opt. Soc. Am. B **10**, 314 (1993).

[6] A. Figotin and A. Klein, J. Stat. Phys. **86**, 165 (1997).

[7] K. Sakoda and H. Shiroma, Phys. Rev. B **56**, 4830 (1997).

[8] L. I. Deych and A. A. Lisyansky, Bull. Am. Phys. Soc. **42**, 203 (1997); Phys. Lett. A **240**, 329 (1998).

[9] L. I. Deych and A. A. Lisyansky, Phys. Lett. A **243**, 156 (1998).

[10] V. S. Podolsky, L. I. Deych, and A. A. Lisyansky, Phys. Rev. B **57**, 5168 (1998).

[11] There is another type of local photon and polariton states, which must be distinguished from those discussed in the paper. These are so called photon-atom (Refs. 12–14) and polariton-atom (Ref. 15) bound states that arise in both photonic and polariton band gaps due to optically active atom impurities.

[12] S. John and T. Quang, Phys. Rev. A **50**, 1764 (1994).

[13] S. John and J. Wang, Phys. Rev. Lett. **64**, 2418 (1990); Phys. Rev. B **43**, 12 772 (1991).

[14] S. John and T. Quang, Phys. Rev. A **52**, 4083 (1995).

[15] V. I. Rupasov and M. Singh, Phys. Rev. A **54**, 3614 (1996); **56**, 898 (1997).

[16] A. V. Chaplik and M. V. Entin, Zh. Éksp. Teor. Fiz. **67**, 208 (1974) [Sov. Phys. JETP **40**, 106 (1975)].

[17] I. M. Lifshitz and V. Ya Kirpichenkov, Zh. Éksp. Teor. Fiz. **77**, 989 (1979) [Sov. Phys. JETP **50**, 499 (1979)].

[18] R. Bellman and G. Wing, *An Introduction to Invariant Embedding* (Wiley, New York, 1976).

[19] J. C. Penley, Phys. Rev. **128**, 596 (1962).
[20] B. Ricco and M. Ya. Azbel, Phys. Rev. B **29**, 1970 (1984).
[21] V. J. Goldman, D. C. Tsui, and J. E. Cunningham, Phys. Rev. Lett. **58**, 1256 (1987).
[22] V. J. Goldman, D. C. Tsui, and J. E. Cunningham, Phys. Rev. B **35**, 9387 (1987).
[23] A. Zaslavsky, V. J. Goldman, D. C. Tsui, and J. E. Cunningham, Appl. Phys. Lett. **53**, 1408 (1988).